Sensors and Actuators B 245 (2017) 583–589

Contents lists available at ScienceDirect

Sensors and Actuators B: Chemical

journal homepage: www.elsevier.com/locate/snb

High-resolution and temperature-compensational HER2 antigen detection based on microwave photonic interrogation

Yuan Cao [a], Xudong Wang [a], Tuan Guo [a], Yang Ran [a], Xinhuan Feng [a,*], Bai-Ou Guan [a], Jianping Yao [b]

[a] Guangdong Provincial Key Laboratory of Optical Fiber Sensing and Communications, Institute of Photonics Technology, Jinan University, Guangzhou 510632, China
[b] Microwave Photonics Research Laboratory, School of Electrical Engineering and Computer Science, University of Ottawa, Ottawa, Ontario, Canada

ARTICLE INFO

Article history:
Received 13 September 2016
Received in revised form
30 December 2016
Accepted 12 January 2017
Available online 17 January 2017

Keywords:
Microwave photonics
Optical fiber sensor
Fiber grating
Antigen detection

ABSTRACT

The human epidermal growth factor receptor 2 (HER2) is a clinically significant molecular marker of breast cancer. Interrogation of a high-resolution and temperature- compensational HER2 antigen biosensor based on a microwave photonics filter (MPF) is proposed and experimentally demonstrated. A microfiber Bragg grating (mFBG) and a regular fiber Bragg grating (FBG) are used as a sensing probe for HER2 antigen-antibody specific binding detection and for temperature compensation, respectively. The key point of this work is to use the frequency domain interrogation scheme based on an MPF for high resolution biosensing detection. Experimental results show that the frequency shift of an MPF notch has a linear relationship with the surrounding refractive index (SRI) change over a range from 1.332 to 1.352, with an SRI resolution up to 2.45×10^{-6} RIU, which is almost three orders of magnitude better than that based on the conventional wavelength interrogation technology (2.9×10^{-3} RIU) using the same sensing probe. In situ monitoring is achieved with a limit of detection (LOD) up to 50 ng/mL, with temperature self-compensation ability. The proposed frequency-domain interrogation method based on microwave photonics opens up a new way for fiber-optic biochemical and environmental measurement.

1. Introduction

Breast cancer is the most common cancer in women and has the second high mortality rate among the four major cancers [1–3]. In 2015, the mortality rate has increased to 17.4% as reported by the North American Association of Central Cancer Registries (NAACCR) [4], while the number of fatalities due to late disease detection is still increasing. The early diagnosis of breast cancer is important to patient survival, enhancement of therapeutic effectiveness and preventing the relapse [5]. The analysis of biomarkers in blood or inside the cancer cells is one of the methods applied in early diagnosis [5,6]. The human epidermal growth factor receptor 2 (HER2) [6–8] is a clinically significant molecular marker of breast cancer for its association with malignant breast cancer tumor and the high relapse rate in cancer patients [7,8]. Biosensors provide real-time affinity reaction for biomarker analysis compared with the expensive and time consuming commercial platforms using fluorescence labels program and show potentials in label-free detection [9–11].

Optical fiber biosensors offer many advantages due to their high sensitivity, compact size, immunity to electromagnetic interference, and have shown good potential in biomolecules monitoring [12–16]. Nowadays biomolecule detection by measuring the change of surrounding refractive index (SRI) using an interferometer, a fiber grating, optical couplers, or a surface plasmon resonance (SPR) element has been a topic of interest. A conventional optical fiber biosensor is usually implemented based on wavelength monitoring using an optical spectrum analyzer (OSA), but the detecting resolution is limited due to the limited resolution of an OSA (an OSA can normally provide a best resolution of 10^{-2} nm). To distinguish small SRI variation induced by biochemical reaction, optical fiber sensors with higher SRI sensitivity and the associated interrogation solutions with better resolution are necessary. In addition, biochemical reactions are usually accompanied with thermal changes which will highly affect the accuracy and stability of the sensing output [17,18]. Therefore, designing a biosensor with a higher resolution that is not sensitive to temperature change is an important topic in this field.

A microwave photonic filter (MPF) is a device that is able to process high-frequency and wide-bandwidth microwave signals directly in the optical domain [19–21]. Besides the applications

* Corresponding author.
E-mail address: eexhfeng@gmail.com (X. Feng).

http://dx.doi.org/10.1016/j.snb.2017.01.085
0925-4005/

in optical communications and radar systems, an MPF has potential applications in high accuracy sensing systems [22–24]. The fundamental concept of using an MPF for high accuracy sensing is to translate the wavelength change in the optical domain to microwave spectrum change in the electrical domain with a significantly improved resolution. In this paper, we propose and experimentally demonstrate a temperature-compensational HER2 antigen sensing system with the interrogation implemented using an MPF with a significantly increased resolution. A surface functionalized microfiber Bragg grating (mFBG) cascaded with a regular fiber Bragg grating (FBG) are used as a sensing element and a temperature-compensation element for biosensing and temperature compensation, respectively, and the interrogation of the sensor is achieved by translating the wavelength shift of the mFBG due to the SRI change to the microwave spectrum change of an MPF. The proposed HER2 antigen sensor is experimentally demonstrated. The in situ monitoring of the HER2 specific binding reaction process is realized and the HER2 antigen targets diagnose with two different concentrations is confirmed. An increased resolution that is three orders of magnitude better than that based on the conventional wavelength interrogation technology is realized.

2. Principle and experimental setup

2.1. Sensing system

The biomedical sensing system is implemented using an mFBG and a regular FBG, as a sensing element and a temperature-compensation element, that are cascaded in a fiber ring laser cavity to generate two wavelengths, which are used as a dual-wavelength light source to implement a 2-tap MPF. The interrogation is implemented by monitoring the notch frequency shift of the spectral response of the 2-tap MPF. Fig. 1 shows the experimental setup. It consists of an mFBG which is used as an SRI sensing probe, and a regular FBG for temperature compensation (a regular FBG is not sensitive to SRI change, but an mFBG and an FBG show the same temperature sensitivity). The use of the mFBG and the regular FBG in a ring cavity would form a dual-wavelength erbium-doped fiber ring laser (EDFL), with the two lasing wavelengths determined by the center wavelengths of the mFBG and the regular FBG. An erbium-doped fiber amplifier (EDFA) is used in the ring cavity to provide an optical gain. Two polarization controllers (PC1, PC2) and a polarizer are used to introduce nonlinear polarization rotation (NPR) effect to realize multi-wavelength lasing [25]. An optical coupler (OC1) in the ring cavity is used to couple 20% of the lasing light out of the ring cavity and sent via a second optical coupler (OC2, 99% port) to a single-sideband (SSB) modulator. A third PC (PC3) is used before the SSB modulator to minimize the polarization-dependent loss. The light from the 1% port of OC2 is sent to an OSA (YOKOGAWA AQ6370B) for optical spectrum monitoring.

The SSB modulator is driven by an RF signal from a vector network analyzer (VNA: Agilent PN N5222A), to generate a dual-wavelength SSB modulated optical signal, which is sent to a 10-km single-mode fiber (SMF) acting as a wideband dispersive element, to introduce a time delay difference between the two wavelengths (corresponding to two taps – the probe tap and the reference tap). The time-delayed optical signals are detected at a photodetector (PD) and sent back to the VNA, to measure the frequency response of the MPF. The normalized frequency response of the MPF can be expressed as

$$H(f) = r(A_p + A_r \cdot e^{-i2\pi f \Delta T}), \tag{1}$$

where $\Delta T = DL(\lambda_r - \lambda_p)$ is the time delay difference between the probe tap and the reference tap, λ_p and λ_r are the wavelengths of the probe light and the reference light, respectively, $D = 17$ ps/km/nm is the dispersion coefficient of the SMF for the optical carrier wavelength around 1550 nm, L is the length of the SMF, r is the normalization coefficient, and A_p and A_r are the tap coefficients that are related to the optical powers of the probe light and reference light, respectively. The free spectral range (FSR) of the proposed MPF-based sensing system is inversely proportional to the time delay difference and is given by

$$FSR = \frac{1}{\Delta T} = \frac{1}{(\lambda_r - \lambda_p) \cdot D \cdot L} = \frac{1}{\Delta\lambda \cdot D \cdot L}, \tag{2}$$

where $\Delta\lambda = \lambda_r - \lambda_p$ is the wavelength spacing between the probe light and the reference light. The change in SRI will affect the evanescent field distribution and lead to a wavelength shift of probe light. When the alteration is relatively small compared with $\Delta\lambda$ itself, the derivative of the *FSR* with respect to $\Delta\lambda$ can be expressed as

$$d(FSR) = -\frac{d(\Delta\lambda)}{(\Delta\lambda)^2 \cdot D \cdot L} = -\frac{d(\lambda_r - \lambda_p)}{(\Delta\lambda)^2 \cdot D \cdot L} = \frac{d\lambda_p - d\lambda_r}{(\Delta\lambda)^2 \cdot D \cdot L}, \tag{3}$$

where $d\lambda_p$ is the differential of λ_p and $d\lambda_r$ is the differential of λ_r. Note that the mFBG is sensitive to both the temperature and the SRI while the regular FBG is only sensitive to the temperature. Thus, $d\lambda_p$ and $d\lambda_r$ can be written as

$$d\lambda_p = \frac{\partial\lambda_p}{\partial n_{RI}} \cdot dn_{RI} + \frac{\partial\lambda_p}{\partial T} \cdot dT \quad \text{and} \quad \mathrm{d}\lambda_r = \frac{\partial\lambda_r}{\partial T} \cdot \mathrm{dT}, \tag{4}$$

where dn_{RI} is the differential of the SRI and dT is the differential of the temperature. The differential of λ_p consists of two terms that are proportional to dn_{RI} and dT, while the differential of λ_r consists of only one term that is proportional to dT. The difference between $\partial\lambda_p/\partial T$ and $\partial\lambda_r/\partial T$ can be ignored for the mFBG and FBG have the same thermal expansion coefficient since both are made of quartz material. Thus the Eq. (3) can be written as

$$d(FSR) = \frac{1}{(\Delta\lambda)^2 \cdot D \cdot L} \cdot \left(\frac{\partial\lambda_p}{\partial n_{RI}} \cdot dn_{RI} \right) = \frac{-d(\Delta\lambda)}{(\Delta\lambda)^2 \cdot D \cdot L}. \tag{5}$$

Therefore, the change of the FSR is only proportional to the SRI-induced wavelength spacing change, while the influence of the temperature vibration can be ignored. By monitoring the change of the spectral response of the MPF, the sensing information is obtained. A simple way to monitor the change of the spectral response is to monitor the frequency shift of a notch. For example, for the *n-th* order notch, the frequency of the notch is given by

$$f_n = (n - 0.5)FSR = \frac{(n - 0.5)}{\Delta\lambda \cdot D \cdot L} \tag{6}$$

Taking the resolutions of the OSA and the VNA (R_{OSA} is the wavelength demodulation resolution of the OSA and R_{VNA} is the frequency demodulation resolution of the VNA) into consideration, the sensing resolutions of the wavelength demodulation method (r_λ) and the MPF-based demodulation method (r_f) can be expressed as

$$r_\lambda = \frac{d(\Delta\lambda)}{R_{OSA}} \quad \text{and} \tag{7.1}$$

$$r_f = \frac{(n - 0.5)}{(\Delta\lambda)^2 DL} \cdot \frac{d(\Delta\lambda)}{R_{VNA}} \tag{7.2}$$

Note that the term $(n\text{-}0.5)/(\Delta\lambda)^2 DL$ in r_f is of the order of magnitude of about 10^{-2}, while there is a huge difference between R_{OSA} (of the order of magnitude of 10^9 Hz) and R_{VNA} (of the order of magnitude of 10^1–10^5 Hz), thus the MPF-based sensing system has a much higher sensing resolution than that based on the conventional wavelength demodulation using an OSA. The sensing resolution can also be adjusted by choosing the wavelength spacing between the cascaded FBGs or tuning the time delay difference by controlling the

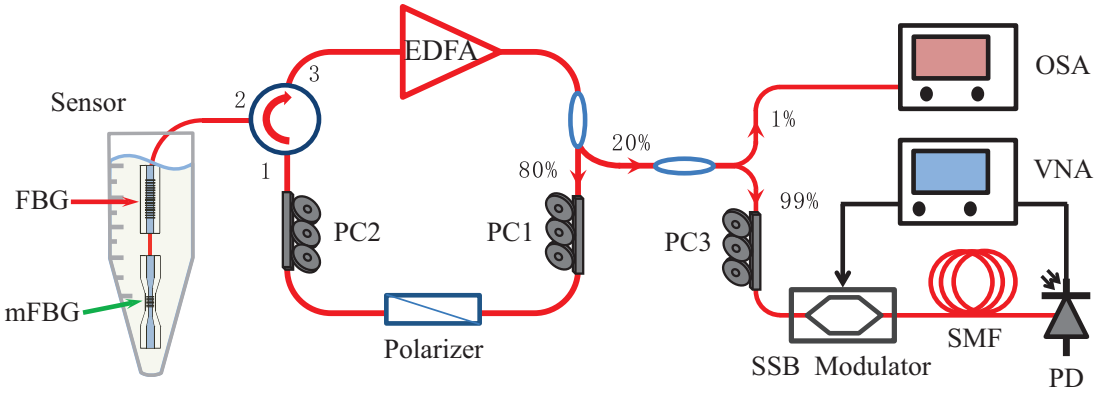

Fig. 1. The experimental setup of the proposed MPF-based biosensing system.

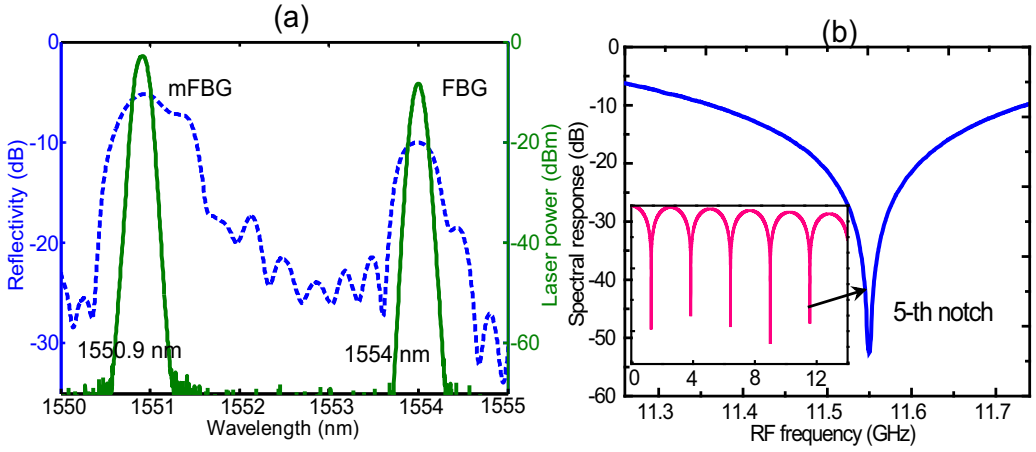

Fig. 2. (a) The reflection spectrum of the mFBG and the regular FBG (dotted blue line) when both are in air and the lasing spectrum at the output of the ring laser (solid green line). (b) The corresponding spectral response of the MPF zoomed at the 5-th notch. The inset shows the spectral response from 0 to 14 GHz. (For interpretation of the references to colour in this figure legend, the reader is referred to the web version of this article.)

length of the dispersive fiber. It should also be noted that the sensing resolution can be further improved by using a higher order notch which is more sensitive to the SRI.

2.2. Sensor fabrication and characterization

The microfiber used to inscribe the mFBG is a commercial multimode fiber drawn and tapered by butane flame brushing. The mFBG is inscribed using a 193-nm ArF excimer laser with a phase mask having a period of 1078.78 nm. The regular FBG is inscribed in an SMF with a phase mask having a period of 1073.81 nm. The center wavelength of the mFBG and normal FBG are 1550.9 nm and 1554 nm, respectively when both FBGs are placed in air. The reflection spectrum of the cascaded mFBG and regular FBG is shown in Fig. 2(a), as the dotted blue curve, in which the left peak corresponds to the center wavelength of the mFBG and the right peak corresponds to the center wavelength of the regular FBG. Since the diameter distribution of the microfiber is not uniform, the 3-dB bandwidth of the reflection spectrum of the mFBG is broader than that of the regular FBG. When the mFBG and the regular FBG are incorporated in the ring cavity, and the gain of the EDFA is sufficiently high, the ring laser starts to lase. The lasing spectrum is also shown in Fig. 2(a), as solid green curve. The spectral response of the MPF (when the mFBG and the regular FBG are in air) zoomed at the 5-*th* notch is shown in Fig. 2(b) as the solid blue curve. The frequency response of the MPF from 0 to 14 GHz is also shown in Fig. 2(b), as an inset.

The SRI sensing characteristics of the proposed sensor using conventional wavelength monitoring and the proposed MPF-based interrogation are carried out by immersing the sensing probe into the sodium chloride solution. The change of the SRI is achieved by adjusting the concentration of the sodium chloride solution through mixing high concentration sodium chloride solution with deionized water. The variation range of the SRI is from 1.332 to 1.352 which is controlled to match the SRI in a bio internal environment. In the experiment, the SRI is measured by recording the frequency of a notch in the frequency response of the MPF. Here the 5-*th* notch is selected. The resolution of the VNA is set to 625 kHz. The SRI sensing characteristics of the MPF-based sensing system and a system based on wavelength monitoring using an OSA (resolution 0.02 nm) are shown in Fig. 3.

For the method based on wavelength monitoring using an OSA, there is a negative correlation between the wavelength spacing and the SRI because the probe wavelength is smaller than the reference wavelength. For the MPF-based biosensing system, there is a positive correlation between the wavelength spacing and the SRI, and the SRI sensitivity after linear fitting is estimated to be 255.26 GHz/RIU. Taking the VNA resolution (625 kHz) into consideration, the SRI sensing resolution of the MPF-based sensing system is 2.45×10^{-6} RIU. The comparison of the SRI sensing resolutions between the OSA-based wavelength monitoring method and the MPF-based frequency monitoring method is shown in Table 1.

It can be seen that the SRI resolution of the MPF-based sensing system is almost three orders of magnitude higher than that

Table 1
Resolution comparison between the OSA-based wavelength monitoring method and the MPF-based frequency monitoring method.

	Sensitivity	Analyzer resolution	Sensing resolution
OSA-based wavelength monitoring	6.8678 nm/RIU	0.02 nm	2.91×10^{-3} RIU
MPF-based frequency monitoring	255.26 GHz/RIU	625 kHz	2.45×10^{-6} RIU

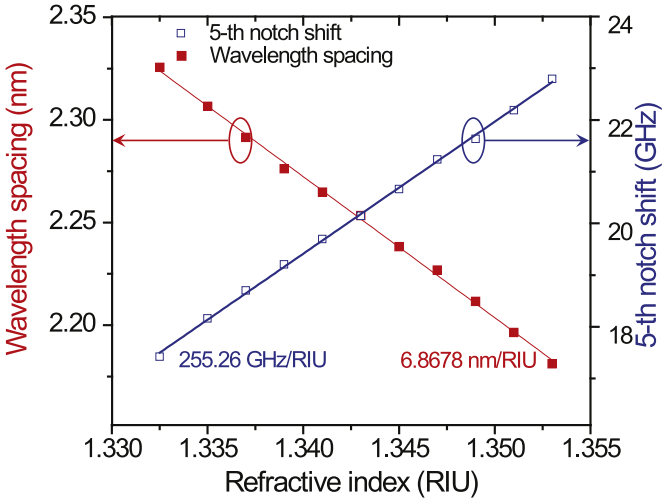

Fig. 3. The SRI sensing characteristics of the biosensor interrogated in the wavelength domain using an OSA (solid square) and the frequency domain (open square) based on an MPF.

of the OSA-based wavelength monitoring method (by using the same sensor probe) due to the higher resolution of the VNA, while the resolution of the same biosensor interrogated based on optical wavelength monitoring is limited by the resolution of the OSA (0.02 nm). The sensitivity of the MPF-based sensing system will increase when measuring the frequency shift of a higher order notch. The sensing resolution can be further improved by setting the VNA at a higher resolution (but the sensing speed may be reduced).

2.3. Sensor surface modification and stability

The immobilization of HER2 antibody molecules is realized by the covalent linking method which has shown good reproducibility [13]. In the preprocessing step, the piranha solution (prepared by mixing 98% sulfuric acid and 30% hydrogen peroxide with a volume ratio of 7:3) is used to clean the surface of the biosensing component (both the mFBG and FBG) for half an hour and also to produce a negatively-charged surface. Fig. 4(a) shows the surface modification procedure and the frequency shift of the MPF notch in each step in the experiment. First, the biosensing component is immersed into the 3-aminopropyl triethoxysilane solution (APTES, 5% v/v in ethanol) for an hour to build up an aminosilane layer on the fiber surface and realize the silanization of the senor component. Then, the fiber senor component is immersed into the glutaraldehyde aqueous solution (10% v/v in water) for half an hour to crosslink the aminated fiber surface. Finally, the fiber senor component is immersed into the HER2 antibody in a phosphate buffered solution (PBS, 250 ng/mL, 5% w/v) for an hour to immobilize the probe molecule layer on the surface of the fiber. After each step above, the sensor component is rinsed by deionized water to remove the unbound or loosely bound reagent molecules on the HER2 antibody layer. The surface immobilized sensor is immersed in the HER2 antigen sample to monitor the specific binding process.

To investigate the stability of the MPF-based biosensing system, the sensing probe is immersed into deionized water for 80 min and the frequency shift of the 5-*th* notch is recorded. The fluctuation of the notch frequency shift versus time is shown in Fig. 4(b). The fluctuation of the notch frequency is within 2.7 MHz. Taking the VNA resolution of 625 kHz into consideration, the fluctuation of the biosensing system is small and acceptable. The x-y transpose curve of the MPF frequency response around the 5-*th* notch is shown in Fig. 4. The 3-dB notch width of the 5-*th* notch is 26 MHz, which is almost 10 times higher than the frequency fluctuations of the notch. Thus, the proposed biosensing system is proved to have a stable operation.

3. Results and discussion

3.1. HER2 specific binding monitoring

The specific binding process of HER2 antibody and antigen is investigated by using the MPF-based frequency monitoring method, and the performance is compared with the conventional wavelength monitoring method. The concentrations of the HER2 antigen are 250, 50 and 10 ng/mL, and from each concentration the experiment is repeated three times. The nonspecific binding experiments under the concentration of 250 ng/mL with immunoglobulin G (IgG) and mouse monoclonal antibody (MAb) are also given. The frequency shift of the 5-*th* notch (monitored by the VNA) and the change of the wavelength spacing (monitored by the OSA) are both recorded and then subtracted by their initial values (the notch frequency and the wavelength spacing in deionized water after the surface modification and the rewash step) to achieved the net shifting curves. The mean value and error bars from the standard deviation are produced by running three individual experiments with the same concentration. Fig. 5 shows the HER2 specific binding and nonspecific group sensing monitoring net shifting curves with the MPF-based frequency monitoring method and conventional wavelength monitoring method.

At a concentration of 250 ng/mL, the net frequency shift of the notch is changing positively during the sensing monitoring process. The HER2 specific binding process includes a rapid reaction occurred in the first 5 min, showing a notch frequency shift rate of 8.3×10^7 Hz/min and a much slower reaction process with a rate of 1.2×10^6 Hz/min from 5 to 60 min as shown in Fig. 5(a). The whole specific binding reaction process is completed in approximately 20 min and the frequency of the notch is then kept constant. The two specific binding processes can be discriminated by the MPF-based frequency monitoring method.

The red curve in Fig. 5(b) shows the sensing process by the conventional wavelength monitoring method. The net wavelength spacing shift is negative and kept declining. Apparently, the conventional wavelength monitoring method cannot monitor the HER2 specific binding reaction. The comparison of the net frequency and wavelength spacing shifts and shift point numbers between the MPF-based frequency monitoring method and the conventional wavelength monitoring method are shown in Table 2. Here the net shift point number is defined as the ratio between the net shift amount and the analyzer resolution.

The net shift point number is positively correlated with the sensing ability of the biosensing system. The net shifting point number of the MPF-based sensing system is almost three orders of magnitude higher than the conventional wavelength monitoring method, which agrees with the SRI sensing resolution comparison between the two different methods as discussed in Table 2. At a concentra-

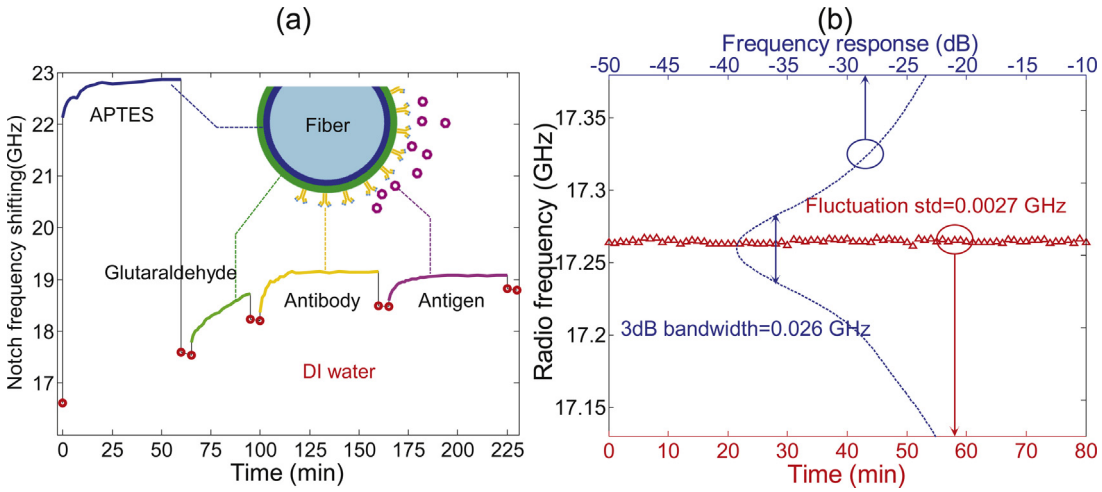

Fig. 4. (a) The surface modification procedure and the frequency shift of the MPF notch in each step (blue line: APTES, green line: glutaraldehyde, yellow line: antibody, purple line: antigen, red dot: deionized water). (b)The fluctuation of the 5-*th* notch point frequency (red triangle) and the x-y transpose MPF frequency response in partial enlarged view around notch point (dashed blue line). (For interpretation of the references to colour in this figure legend, the reader is referred to the web version of this article.)

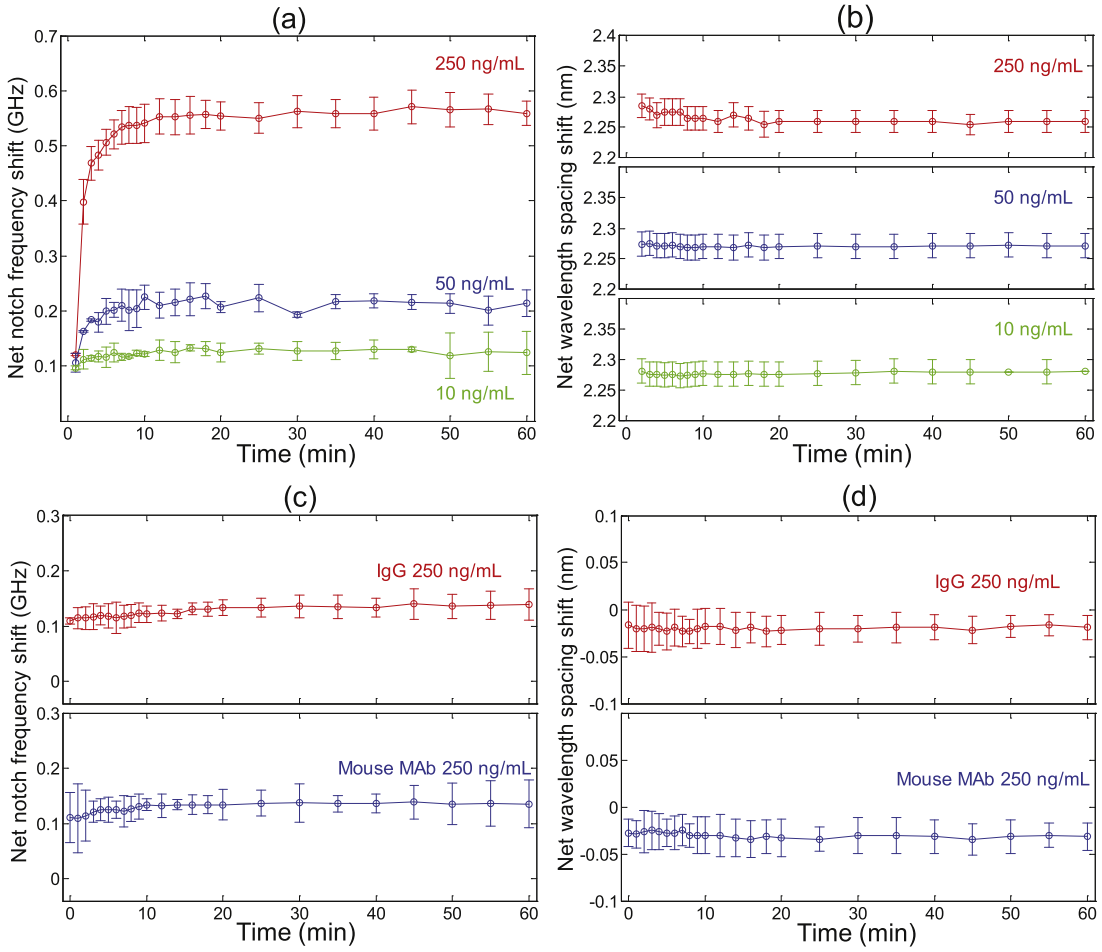

Fig. 5. (a) The HER2 specific binding monitoring curves by the MPF-based frequency monitoring method with 3 concentrations (red line: 250 ng/mL, blue line: 50 ng/mL, green line: 10 ng/mL). (b) The corresponding specific binding monitoring curves by the conventional wavelength monitoring method. (c) The nonspecific monitoring curves by the MPF-based frequency monitoring method with a concentration of 250 ng/mL (red line: IgG, blue line: Mouse MAb). (d) The corresponding nonspecific monitoring curves by the conventional wavelength monitoring method. (For interpretation of the references to colour in this figure legend, the reader is referred to the web version of this article.)

tion of 50 ng/mL, the net frequency shift based on the MPF-based sensing system, shown as blue curve in Fig. 5(a), decreases a lot but the variation trend is still available for biosensing function. As to the conventional wavelength monitoring method, shown as blue

Table 2
Net frequency and wavelength spacing shifts and shift point numbers between the MPF-based frequency monitoring method and the conventional wavelength monitoring method at a concentration of 250 ng/mL.

	Net shift amount	Analyzer resolution	Shift point number
OSA-based wavelength monitoring	0.405 nm	0.02 nm	2.25
MPF-based frequency monitoring	450 MHz	625 kHz	720

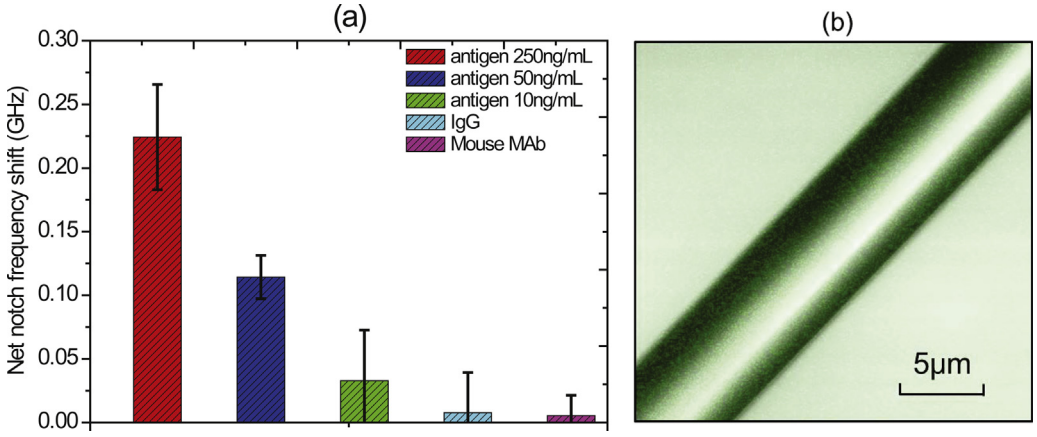

Fig. 6. (a) The detection result at different concentrations (red column for antigen with 250 ng/mL, blue column for antigen with 50 ng/mL and green column for antigen with 10 ng/mL) and the nonspecific binding detection (light blue column for IgG and purple column for mouse MAb); (b) The confocal microscopy image of the mFBG surface after specific binding detection with fluorescein isothiocyanate (FITC) marked HER2 antigen. (For interpretation of the references to colour in this figure legend, the reader is referred to the web version of this article.)

curve in Fig. 5(b), the decline trend of the wavelength spacing is not obvious and is covered by the error bars, which means the sensing function is failed.

The green curves in Fig. 5(a) and (b) show the sensing curves at a concentration of 10 ng/mL by the MPF-based sensing system and by the conventional wavelength monitoring method, respectively. The sensing curves for both methods are random and covered by their own error bars. Neither of them is able to recognize the HER2 specific binding reaction. The nonspecific binding experiments under a high concentration (250 ng/mL) with IgG and mouse MAb are shown in Fig. 5(c) and (d). The variation trend in the monitoring curve for both MPF-based sensing system and the conventional wavelength monitoring method are not obvious, which means the selectivity of the biosensing system is reliable.

3.2. HER2 detection result

To investigate the HER2 detection ability of the proposed MPF-based sensing system, we record the notch frequency after the surface modification step and after the specific binding reaction step (the sensor component is in deionized water). The concentrations of the HER2 antibody in the surface modification step are all set to 250 ng/mL. The mean value and error bars of the net shift are calculated and the detection resulting histograms with standard deviation at different concentrations are shown in Fig. 6(a).

For HER2 antigen at 250 ng/mL (red column), the mean value and the standard deviation of the net frequency shift of the 5-*th* notch frequency are 224 MHz and 41 MHz, respectively. It is sufficient to distinguish the frequency difference between the surface modification step and the specific binding reaction step, and the HER2 antigen can be affirmed. For 50 ng/mL (blue column), the mean value and the standard deviation of the net frequency shift of the 5-*th* notch frequency are 114 MHz and 17 MHz, respectively, and the net frequency shift detecting result is lower than that in a high concentration. There is no overlapping between the error bars in 250 ng/mL and 50 ng/mL, which means that the HER2 antigen can be marked for those 2 concentrations. While for 10 ng/mL (green column), the mean value is 33 MHz which is at the same level (or even lower than) as that of the standard deviation (40 MHz) of the net frequency shift of the notch frequency, resulting in an invalid detection. Therefore, the experimental results show that the LOD of our proposed sensing system for HER2 antigen detection is at a level of 50 ng/mL in concentration. For nonspecific binding detections, the mean values for IgG and mouse MAb (around 6 MHz) are lower than that of the low concentration antigen (41 MHz). The standard deviations are 31 MHz and 16 MHz for IgG and mouse Mab, respectively, which are even higher than their mean value. Fig. 6(b) shows the confocal microscopy image of the mFBG surface after specific binding detection with fluorescein isothiocyanate (FITC) marked HER2 antigen (250 ng/mL) with a 448 nm laser source for the excitation, in which the specific binding process can be confirmed.

4. Conclusion

We have demonstrated a high resolution and temperature compensational biosensor for HER2 antigen detection based on monitoring the spectrum of an MPF. A surface functionalized mFBG cascaded with normal FBG was used as the biosensing probe to realize in-situ detection. The MPF-based SRI sensing system provides an improved resolution of 2.45×10^{-6} RIU which is three orders of magnitude higher than a conventional optical wavelength monitoring method. The surface functionalization of the biosensing component was covalent linking method and the operation stability of the biosensing system was qualified. The HER2 specific binding reaction process was in situ monitored clearly by the MPF-based frequency monitoring method. The proposed sensing method can achieve HER2 antigen detection with LOD of 50 ng/mL in concentration, making it a good candidate for preliminary diagnosis of breast cancers.

Acknowledgements

This work was supported in part by the National Natural Science Foundation of China (No. 61475065, No. 61501205), the

Guangdong Natural Science Foundation (No. 2015A030313322, No. 2014A030313387, No. 2014A030310419), the Guangdong Youth Science and Technology Innovation Talents of China (No. 2014TQ01X539), the Guangdong Innovation Foundation of China (No. 2015KTSCX016) and the Guangzhou Key Collaborative Innovation Foundation of China (No. 2016201604030084).

References

[1] H.D. Cheng, J. Shan, W. Ju, Y. Guo, L. Zhang, Automated breast cancer detection and classification using ultrasound images: a survey, Pattern Recogn. 43 (2009) 299–317.
[2] M.E. Lippman, Harrison's Principles of Internal Medicine, McGraw-Hill, Medical Publishing Division, 2008, 2017.
[3] A. Jemal, R. Siegel, E. Ward, T. Murray, J. Xu, C. Smigal, M.J. Thun, Cancer statistics, CA Cancer J. Clin. 56 (2006) 106–130.
[4] R.L. Siegel, K.D. Miller, A. Jemal, Cancer statistics, CA Cancer J. Clin. 65 (2015) 5–29.
[5] A.J. Kearney, M. Murray, Breast cancer screening recommendations: is mammography the only answer? J. Midwifery Women Health 54 (2009) 393–400.
[6] L.W.J. Gullick, Update on HER-2 as a target for cancer therapy: alternative strategies for targeting the epidermal growth factor system in cancer, Breast Cancer Res. 3 (2001) 390–394.
[7] G. Riccio, G. Esposito, E. Leoncini, R. Contu, G. Condorelli, M. Chiariello, P. Laccetti, S. Hrelia, G. D'Alessio, C. De Lorenzo, Cardiotoxic effects or lack thereof, of anti-ErbB2 immunoagents, FASEB J. 23 (2009) 3171–3178.
[8] H. Cho, K. Mason, K.X. Raymer, A.M. Stanley, S.B. Gabelli, D.W. Denney, D.J. Leahy, Structure of the extracellular region of HER2 alone and in complex with the Herceptin Fab, Nature 421 (2003) 756–760.
[9] R.D. Mass, M.F. Press, S. Anderson, M.A. Cobleigh, C.L. Vogel, N. Dybdal, G. Leiberman, D.J. Slamon, Evaluation of clinical outcomes according to HER2 detection by fluorescence in situ hybridization in women with metastatic breast cancer treated with trastuzumab, Clin. Breast Cancer 6 (2005) 240–246.
[10] J.A. Ramos-Vara, Technical aspects of immunohistochemistry, Vet. Pathol. 42 (2005) 405–426.
[11] H. Mukundan, J.Z. Zubicek, A. Holt, J.E. Shively, J.S. Martinez, K. Grace, W.K. Grace, B.I. Swanson, Planar optical waveguide-based biosensor for the quantitative detection of tumor markers, Sens. Actuators B: Chem. 138 (2009) 453–460.
[12] J.W. Chung, R. Bernhardt, J.C. Pyun, Additive assay of cancer marker CA 19-9 by SPR biosensor, Sens. Actuators B: Chem. 118 (2006) 28–32.
[13] J.T. Gohring, P.S. Dale, X. Fan, Detection of HER2 breast cancer biomarker using the opto-fluidic ring resonator biosensor, Sens. Actuators B: Chem. 146 (2010) 226–230.
[14] D.W. Kim, Y. Zhang, K.L. Cooper, A. Wang, Fibre-optic interferometric immuno-sensor using long period grating, Electron. Lett. 42 (2006) 324–325.
[15] J.M. Corres, I.R. Matias, J. Bravo, F.J. Arregui, Tapered optical fiber biosensor for the detection of anti-gliadin antibodies, Sens. Actuators B: Chem. 135 (2008) 166–171.
[16] Y. Cao, T. Guo, X. Wang, D. Sun, Y. Ran, X. Feng, B.O. Guan, Resolution-improved in situ DNA hybridization detection based on microwave photonic interrogation, Opt. Exp. 23 (2015) 27061–27070.
[17] J.M. Sturtevant, Heat capacity and entropy changes in processes involving proteins, Proc. Natl. Acad. Sci. 74 (1977) 2236–2240.
[18] P.D. Ross, S. Subramanian, Thermodynamics of protein association reactions: forces contributing to stability, Biochemistry 20 (1981) 3096–3102.
[19] J. Capmany, B. Ortega, D. Pastor, A tutorial on microwave photonic filters, J. Lightw. Technol. 24 (2006) 201–229.
[20] R.A. Minasian, Photonic signal processing of microwave signals, IEEE Trans. Microw. Theory Tech. 54 (2006) 832–846.
[21] J. Yao, Microwave photonics, J. Lightw. Technol. 27 (2009) 314–335.
[22] X. Dong, L.Y. Shao, H. Fu, H. Tam, C. Lu, Intensity-modulated fiber Bragg grating sensor system based on radio-frequency signal measurement, Opt. Lett. 33 (2008) 482–484.
[23] W. Liu, H. Fu, A.P. Zhang, S. He, Fiber Bragg grating based wireless sensor module with modulated radio-frequency signal, IEEE Microw. Wirel. Compon. Lett. 20 (2010) 358–360.
[24] A. Ricchiuti, D. Barrera, S. Sales, L. Thevenaz, J. Capmany, Long weak FBG sensor interrogation using microwave photonics filtering technique, IEEE Photonics Technol. Lett. 26 (2014) 2039–2042.
[25] X. Feng, H.-Y. Tam, P. Wai, Stable and uniform multiwavelength erbium-doped fiber laser using nonlinear polarization rotation, Opt. Exp. 14 (2006) 8205–8210.

Biographies

Yuan Cao received the B.S. degree from Dalian University of Technology, Dalian, China, in 2011, and the Ph.D. degree from Jinan University, Guangzhou, China, in 2016. He is currently a lecturer at the Institute of Photonics Technology, Jinan University, Guangzhou, China. His research interests include microwave photonics signal processing & applications and optical biosensors.

Xudong Wang received the B.E. degree in electrical engineering from Dalian University of Technology, Dalian, China, in 2007, the M.E. and Ph.D. degrees from the University of Sydney, Australia, in 2008 and 2014, respectively. He is currently a lecturer in the Institute of Photonics Technology, Jinan University, China. His research interest is microwave photonic signal processing.

Tuan Guo is a Professor in the Institute of Photonics Technology, Jinan University, Guangzhou, China. He received the B.Sc. and the M.Sc. in Electrical Engineering from Xi'an Shiyou University in 2001 and 2004, and the Ph.D. in Optics from Nankai University in 2007. Thereafter he worked as a Postdoctoral Fellow with the Department of Electronics at Carleton University (Canada) and the Photonics Research Centre at The Hong Kong Polytechnic University. He joined the Jinan University as an Associate Professor in 2011 and promoted to a full Professor in 2014. He has authored or coauthored over 100 peer-reviewed journal articles mainly in *Biosensors and Bioelectronics, Analytical Chemistry, Analytical and Bioanalytical Chemistry, Applied Physics Letters, Optics Letters, Optics Express and IEEE series*. He holds 15 patents and pending patents. His research activities include optical fiber sensors, fiber lasers, fiber gratings, plasmonics, biophotonics, microfluidic and microcavity devices He was an Associated Editor for *Journal of Sensors* from 2010 to 2014 and a Guest Editor for a Special Issue on "Recent Advances in Fiber Bragg Grating Sensing" in MDPI Sensors in 2016. He is a member of the IEEE and the Optical Society of America (OSA).

Yang Ran received the B.S. degree from Dalian University of Technology, Dalian, China, in 2006, and the Ph.D. degree from Jinan University, Guangzhou, China, in 2013. He is currently a lecturer at the Institute of Photonics Technology, Jinan University, Guangzhou, China. His research interests include optical fiber devices & sensors and optical bio-medical sensors.

Xinhuan Feng received the B.Sc degree at physics department of Nankai University in 1995, and obtained her M.Sc and Ph.D degrees respectively in 1998 and 2005 at Institute of Modern Optics, Nankai University, China. From 2005–2008, she worked as a postdoctoral fellow at Photonics Research Centre of the Hong Kong Polytechnic University. Since March 2009, she has been with the Institute of Photonics Technology, Jinan University, China. Her research interests include various fiber active and passive devices and their applications, and microwave photonic signal processing.

Bai-Ou Guan received the B.Sc. degree in applied physics from Sichuan University, Chengdu, China, in 1994, and the M.Sc. and Ph.D. degrees in optics from Nankai University, Tianjin, China, in 1997 and 2000, respectively. From 2000–2005, he was with the Department of Electrical Engineering, the Hong Kong Polytechnic University, Hong Kong, first as a Research Associate, then as a Postdoctoral Research Fellow. From 2005–2009, he was with School of Physics and Optoelectronic Engineering, Dalian University of Technology, Dalian, China, as a Full Professor, where he established the PolyU-DUT Joint Research Center for Photonics. In 2009, he joined Jinan University, Guangzhou, China, where he founded the Institute of Photonics Technology. His current research interests include fiber optic devices and technologies, optical fiber sensors, biomedical photonic sensing and imaging, and microwave photonics. He has authored and coauthored more than 240 technical papers and presented more than 30 invited talks at international conferences. He is a member of OSA and IEEE, and served as the General Chair of the 10th International Conference on Optical Communications and Networks (ICOCN2011), the General Co-Chair of the 2nd Asia-Pacific Optical Sensors Conference (APOS2010), and the Technical Program Committee Co-Chair of the 5th Asia-Pacific Microwave Photonics Conference 2010 (APMP2010).

Jianping Yao is a distingusished University Professor and University Research Chair in the School of Electrical Engineering and Computer Science, University of Ottawa, Canada. Prof. Yao has published over 520 papers in refereed journals and conference proceedings. He is a topical editor for Optics Letters, and serves on the Editorial Boards of Optics Communications and Science Bulletin. Prof. Yao is a Fellow of IEEE, a Fellow of the Optical Society of America, and a Fellow of the Canadian Academy of Engineering.